PHYSICAL REVIEW B VOLUME 50, NUMBER 9 1 SEPTEMBER 1994-I

Domain formation and elastic long-range interaction in ferroelectric perovskites

Shinji Nambu and Djuniadi A. Sagala
Central Research Laboratory, Kyocera Corporation, 1-4 Yamashita-cho, Kokubu, Kagoshima 899-43, Japan
(Received 17 February 1994)

On the basis of a Ginzburg-Landau model for ferroelectric perovskites, we calculate an effective free energy for a polarization field by eliminating elastic fields which are coherently induced by inhomogeneous configurations of polarizations. We obtain elastic long-range interaction between polarization fields on an adiabatic approximation. Computer simulations of a two-dimensional time-dependent Ginzburg-Landau (TDGL) model are performed by taking into account those long-range interactions. Charge-neutral 90° twins and its time evolution in the tetragonal phase are obtained with appropriate parameters of a phenomenological free energy. Resultant domain patterns are in agreement with experimental observations of tetragonal $BaTiO_3$ ceramics. It is shown that anisotropic long-range interaction between polarization fields caused by elastic effects plays a major role in determining both the domain morphology and domain growth law in ferroelectric perovskites.

I. INTRODUCTION

There is considerable interest in ferroelectric transition, in which a long-wavelength instability creates a pattern formation of domains and the domains coarsen and grow to macroscopic size as time evolves. This process is also technologically important, since applications of ferroelectric materials need to control macroscopic characteristics, such as hysteresis loop, dielectric loss, aging phenomena, etc., which relate to the domain morphology and domain motion.[1-4]

Twinning in ferroelectric single crystals may be eliminated by field-induced domain switching. A single crystal has a free boundary condition, it need not have twins in the thermodynamic limit from the mechanical point of view. In a ceramic, a crystallite (one grain) is clamped by its neighboring grains in all three dimensions. Numerous polycrystalline ferroelectrics which undergo the phase transition have a simple lamellar twinning or a complex banded twin structure.[5] Typical examples have been reported for $BaTiO_3$ (Refs. 6–8) and $Pb(Zr,Ti)O_3$ solid solutions.[9-14] The physical origin of these twinning structures, in a static sense, may be ascribed to the sum of electrostatic energy of polarizations and elastic energy, which is reduced at the expense of domain-wall energy in order to minimize the total energy by the formation of twins, although the formation process of these twins is essentially nonequilibrium.

On the basis of studies using electron microscopy,[5-14] our present knowledge of ferroelectric domains in tetragonal $BaTiO_3$ and $Pb(Zr,Ti)O_3$ can be summarized as follows. Two kinds of domains can exist, 90° domain and 180° domain. The predominant category of domains are 90° domains. The adjacent domains of this kind are twin related.[9] The twin boundary is the domain boundary and the twin plates are ferroelectric domains.[8,10,12] The twin planes are $\{110\}$ and the polarization vectors in adjacent domains are perpendicular to each other and adopt a "head-to-tail" arrangement across a 90° boundary in order to minimize the charge at the domain wall. These twins are displacement twins, and are created due to stress in the material during the paraelectric to ferroelectric phase transition.[10] On the other hand, the energy of 180° boundary walls is less sensitive to crystallographic orientation.[8] The electrostatic energy is minimized when the polarization vectors of adjacent domains are adopted such that div $P=0$ at the domain boundary. This is satisfied for 90° and 180° walls. There is no expense of elastic energy for 180° walls. It can be said that 180° walls form to minimize the electrostatic energy, while in 90° domains (twins), elastic energy minimization is predominant. The experimentally observed preponderance of 90° domains show that the effect of elastic strain plays a major role in determining the domain morphology in $BaTiO_3$ and $Pb(Zr,Ti)O_3$.

Cao and Cross[15] proposed a three-dimensional Landau-Ginzburg model to describe the tetragonal twin structures in ferroelectric perovskites, and they presented quasi-one-dimensional analytic solutions for the space profiles of the order parameter for a 180° twin and a charge neutral 90° twin, though the solutions are static for a single domain and they did not treat elastic long-range interactions. From the view point of elastic effect, the situation of ferroelectric 90° twins is analogous to twins in ferroelastic materials which is caused by martensitic transformation.[16,17] The twin bands in martensites is stabilized by a long-range elastic interaction between the twin boundaries.[17] Furthermore, with respect to elastic effect on pattern formation in solids, it has been shown that elastic long-range interactions determined both the domain morphology and domain growth law of spinodal decomposition with the coherence of the lattice based on a time-dependent Ginzburg-Landau (TDGL) model.[18-23] On the formation of ferroelectric domain structure the same situation will be expected.

In the present work we study the dynamics of formation of ferroelectric domain structures with a first-order phase transition on the basis of a TDGL model. We derive an effective free energy for the local polarization field by eliminating elastic fields which are coherently in-

0163-1829/94/50(9)/5838(10)/$06.00

duced by polarization inhomogeneities in Secs. II–IV. A general dynamic equation for the local polarization field to describe the pattern formation of ferroelectric domain structure is presented in Sec. V. Two-dimensional numerical simulations are done in Sec. VI. Summary and conclusions are included in Sec. VII.

II. MODEL FREE ENERGY

The total free energy of the system to describe ferroelectric phase transition is written by a sum of the Landau-Devonshire free-energy density f_p, the elastic free-energy density $f_{\rm el}$, the electrostrictive free-energy density f_c, and the gradient free-energy density f_g:

$$F[\{\mathbf{P}(\mathbf{r})\},\{u_{ij}(\mathbf{r})\}]=\int d\mathbf{r}[f_p+f_{\rm el}+f_c+f_g] , \tag{2.1}$$

where $\mathbf{P}(\mathbf{r})$ is the polarization field and $u_{ij}(\mathbf{r})$ is elastic strain field. The Landau-Devonshire free-energy density is expressed as

$$\begin{aligned} f_p(\{\mathbf{P}\})=&\alpha_1(P_x^2+P_y^2+P_z^2)+\alpha_{11}(P_x^2+P_y^2+P_z^2)^2+\alpha_{12}(P_x^2P_y^2+P_y^2P_z^2+P_z^2P_x^2)+\alpha_{111}(P_x^6+P_y^6+P_z^6)\\ &+\alpha_{112}[P_x^4(P_y^2+P_z^2)+P_y^4(P_z^2+P_x^2)+P_z^4(P_x^2+P_y^2)]+\alpha_{123}P_x^2P_y^2P_z^2 , \end{aligned} \tag{2.2}$$

where α_1 is written as

$$\alpha_1=(2\varepsilon_0 C)^{-1}(T-T_0) \tag{2.3}$$

with Curie constant C and permittivity of vacuum ε_0. The elastic free-energy density of the system is given by

$$f_{\rm el}=2^{-1}C_{11}(u_{xx}^2+u_{yy}^2+u_{zz}^2)+C_{12}(u_{xx}u_{yy}+u_{yy}u_{zz}+u_{zz}u_{xx})+2^{-1}C_{44}(u_{xy}^2+u_{yz}^2+u_{zx}^2) , \tag{2.4}$$

where we use the notation of strain fields $u_{ii}=\partial u_i/\partial x_i$ and $u_{ij}=\partial u_i/\partial x_j+\partial u_j/\partial x_i$ $(i\neq j;i,j=1,2,3)$, $u_i(\mathbf{r})$ is the component of elastic displacement, C_{ij} are the second-order elastic constants. The coupling term between the polarization field and the strain field is written as

$$\begin{aligned} f_c=&-q_{11}(u_{xx}P_x^2+u_{yy}P_y^2+u_{zz}P_z^2)-q_{12}\{u_{xx}(P_y^2+P_z^2)+u_{yy}(P_x^2+P_z^2)+u_{zz}(P_x^2+P_y^2)\}-q_{44}(u_{xy}P_xP_y+u_{yz}P_yP_z+u_{zx}P_zP_x)\\ =&-\sum_{\rho=1}^{6}u_\rho g_\rho , \end{aligned} \tag{2.5}$$

where q_{ij} are the electrostrictive coefficients, and functions g_ρ are defined by

$$g_1=g_{xx}=(q_{11}-q_{12})P_x^2+q_{12}\mathbf{P}^2 , \tag{2.6a}$$

$$g_2=g_{yy}=(q_{11}-q_{12})P_y^2+q_{12}\mathbf{P}^2 , \tag{2.6b}$$

$$g_3=g_{zz}=(q_{11}-q_{12})P_z^2+q_{12}\mathbf{P}^2 , \tag{2.6c}$$

$$g_4=g_{yz}=q_{44}P_yP_z , \tag{2.6d}$$

$$g_5=g_{xz}=q_{44}P_xP_z , \tag{2.6e}$$

and

$$g_6=g_{xy}=q_{44}P_xP_y . \tag{2.6f}$$

We write the gradient free-energy density of the lowest order with cubic symmetry as

$$\begin{aligned} f_g\left[\left\{\frac{\partial P_i}{\partial x_j}\right\}\right]=&\frac{1}{2}G_{11}\left\{\left[\frac{\partial P_x}{\partial x}\right]^2+\left[\frac{\partial P_y}{\partial y}\right]^2+\left[\frac{\partial P_z}{\partial z}\right]^2\right\}\\ &+G_{12}\left\{\left[\frac{\partial P_x}{\partial x}\right]\left[\frac{\partial P_y}{\partial y}\right]+\left[\frac{\partial P_y}{\partial y}\right]\left[\frac{\partial P_z}{\partial z}\right]+\left[\frac{\partial P_z}{\partial z}\right]\left[\frac{\partial P_x}{\partial x}\right]\right\}\\ &+\frac{1}{2}G_{44}\left\{\left[\frac{\partial P_x}{\partial y}+\frac{\partial P_y}{\partial x}\right]^2+\left[\frac{\partial P_y}{\partial z}+\frac{\partial P_z}{\partial y}\right]^2+\left[\frac{\partial P_z}{\partial x}+\frac{\partial P_x}{\partial z}\right]^2\right\}\\ &+\frac{1}{2}G'_{44}\left\{\left[\frac{\partial P_x}{\partial y}-\frac{\partial P_y}{\partial x}\right]^2+\left[\frac{\partial P_y}{\partial z}-\frac{\partial P_z}{\partial y}\right]^2+\left[\frac{\partial P_z}{\partial x}-\frac{\partial P_x}{\partial z}\right]^2\right\} . \end{aligned} \tag{2.7}$$

We assume that the coefficient α_1 is temperature dependent, and others are independent of temperature, which is conventional in Landau theory.

III. FREE ENERGY IN THE STRESS-FREE STATE

We summarize simple expressions of the stress-free state in order to clarify the effect of elastic long-range interactions which is discussed in a later section. The local stress field σ_{ij} is given by

$$\sigma_{xx}=\delta F/\delta u_{xx}=C_{11}u_{xx}+C_{12}(u_{yy}+u_{zz})-g_{xx} , \tag{3.1a}$$

$$\sigma_{yy}=\delta F/\delta u_{yy}=C_{11}u_{yy}+C_{12}(u_{xx}+u_{zz})-g_{yy} , \tag{3.1b}$$

$$\sigma_{zz}=\delta F/\delta u_{zz}=C_{11}u_{zz}+C_{12}(u_{xx}+u_{yy})-g_{zz} , \tag{3.1c}$$

$$\sigma_{yz}=\delta F/\delta u_{yz}=C_{44}u_{yz}-g_{yz} , \tag{3.1d}$$

$$\sigma_{xz}=\delta F/\delta u_{xz}=C_{44}u_{xz}-g_{xz} , \tag{3.1e}$$

$$\sigma_{xy}=\delta F/\delta u_{xy}=C_{44}u_{xy}-g_{xy} . \tag{3.1f}$$

Putting stress field $\sigma_{ij}=0$ in the equilibrium, we have the strain fields of the stress-free state

$$u_{xx}=Q_{11}P_x^2+Q_{12}(P_y^2+P_z^2) , \tag{3.2a}$$

$$u_{yy}=Q_{11}P_y^2+Q_{12}(P_x^2+P_z^2) , \tag{3.2b}$$

$$u_{zz}=Q_{11}P_z^2+Q_{12}(P_x^2+P_y^2) , \tag{3.2c}$$

$$u_{yz}=(q_{44}/C_{44})P_yP_z , \tag{3.2d}$$

$$u_{xz}=(q_{44}/C_{44})P_xP_z , \tag{3.2e}$$

$$u_{xy}=(q_{44}/C_{44})P_xP_y , \tag{3.2f}$$

where we define new constants as follows:

$$Q_{11}=3^{-1}(\hat{q}_{11}/\hat{C}_{11}+2\hat{q}_{22}/\hat{C}_{22}) , \tag{3.3a}$$

$$Q_{12}=3^{-1}(\hat{q}_{11}/\hat{C}_{11}-\hat{q}_{22}/\hat{C}_{22}) , \tag{3.3b}$$

$$\hat{q}_{11}=q_{11}+2q_{12} , \tag{3.3c}$$

$$\hat{q}_{22}=q_{11}-q_{12} , \tag{3.3d}$$

$$\hat{C}_{11}=C_{11}+2C_{12} , \tag{3.3e}$$

$$\hat{C}_{22}=C_{11}-C_{12} . \tag{3.3f}$$

Substitution of Eqs. (3.2a)–(3.2f) into Eqs. (2.4) and (2.5) leads to the effective Landau-Devonshire free-energy density for the stress-free state

$$\begin{aligned} f_{\rm sf}=f_p+f_{\rm el}+f_c=&\alpha_1(P_x^2+P_y^2+P_z^2)+\alpha'_{11}(P_x^2+P_y^2+P_z^2)^2+\alpha'_{12}(P_x^2P_y^2+P_y^2P_z^2+P_z^2P_x^2)+\alpha_{111}(P_x^6+P_y^6+P_z^6)\\ &+\alpha_{112}\{P_x^4(P_y^2+P_z^2)+P_y^4(P_x^2+P_z^2)+P_z^4(P_x^2+P_y^2)\}+\alpha_{123}P_x^2P_y^2P_z^2 , \end{aligned} \tag{3.4}$$

where effective expansion coefficients α'_{11} and α'_{12} are written as

$$\alpha'_{11}=\alpha_{11}-6^{-1}(\hat{q}_{11}^2/\hat{C}_{11}+2\hat{q}_{22}^2/\hat{C}_{22}) , \tag{3.5a}$$

$$\alpha'_{12}=\alpha_{12}-2^{-1}(q_{44}^2/C_{44}-2\hat{q}_{22}^2/\hat{C}_{22}) . \tag{3.5b}$$

The expression of the effective free-energy density of Eq. (3.4) is used to describe the uniform solution of the stress-free state in equilibrium.

IV. ELASTIC LONG-RANGE INTERACTIONS

The static equilibrium conditions can be derived by using variational method.[15] Euler equations are written as

$$\sum_j \frac{\partial}{\partial x_j}\frac{\partial F}{\partial P_{i,j}}-\frac{\partial F}{\partial P_i}=0 \quad (i,j=1,2,3) \tag{4.1a}$$

with $P_{i,j}=\partial P_i/\partial x_j$ and

$$\delta F/\delta u_i=-\sum_j \partial\sigma_{ij}/\partial x_j=0 \quad (i,j=1,2,3) . \tag{4.1b}$$

Equation (4.1b) describes the condition of mechanical equilibrium. In this paper we do not try to solve Eq. (4.1a) analytically in the equilibrium state, but we try to obtain numerical solutions in the nonequilibrium state by a TDGL equation later. Substitution of Eqs. (3.1a)–(3.1f) into Eq. (4.1b) leads to

$$\sum_j \frac{\partial}{\partial x_j}g_{ij}=(C_{11}-C_{12})\frac{\partial u_{ii}}{\partial x_i}+C_{12}\frac{\partial}{\partial x_i}\sum_j u_{jj} +C_{44}\sum_{j(\neq i)}\frac{\partial u_{ij}}{\partial x_j} . \tag{4.2}$$

We define the Fourier transformation of the displacement field $u_i(\mathbf{r})$

$$u_i(\mathbf{k})=(2\pi)^{-d/2}\int d\mathbf{r}\, u_i(\mathbf{r})\exp[-i\mathbf{k}\cdot\mathbf{r}] \tag{4.3}$$

and function $g_{ij}(\mathbf{r})$ is defined by (2.6a)–(2.6f)

$$g_{ij}(\mathbf{k})=(2\pi)^{-d/2}\int d\mathbf{r}\, g_{ij}(\mathbf{r})\exp[-i\mathbf{k}\cdot\mathbf{r}] . \tag{4.4}$$

We obtain the mechanical equilibrium in the Fourier space as

$$(ik^{-1})\sum_j \hat{k}_j g_{ij}(\mathbf{k})+[(C_{11}-C_{12}-2C_{44})\hat{k}_i^2+C_{44}]u_i(\mathbf{k}) +(C_{12}+C_{44})\hat{k}_i\sum_j \hat{k}_j u_j(\mathbf{k})=0 \tag{4.5}$$

with the directional cosines in the Fourier space $\hat{k}_j=k_j/|\mathbf{k}|$ $(j=1,2,3)$, which satisfy $\sum \hat{k}_j^2=1$. Solving Eq. (4.5), we obtain the displacement field in the Fourier space as follows:

$$u_j(\mathbf{k})=-ik^{-1}[G_j(\mathbf{k})/d_j-D(\hat{\mathbf{k}})H(\mathbf{k})\hat{k}_j/d_j] , \tag{4.6}$$

where

$$G_i(\mathbf{k})=\sum_j \hat{k}_j g_{ij}(\mathbf{k}) , \quad (4.7)$$

$$H(\mathbf{k})=\sum_i \hat{k}_i G_i(\mathbf{k})/d_i=\sum_{i,j} \hat{k}_i\hat{k}_j g_{ij}(\mathbf{k})/d_i , \quad (4.8)$$

$$D(\hat{\mathbf{k}})=(C_{12}+C_{44})/[1+(C_{12}+C_{44})\chi(\hat{\mathbf{k}})] , \quad (4.9)$$

$$\chi(\hat{\mathbf{k}})=\sum_j \hat{k}_j{}^2/d_j , \quad (4.10)$$

and

$$d_j=C_{44}[1+\xi\hat{k}_j^2] \quad (4.11)$$

with

$$\xi=(C_{11}-C_{12}-2C_{44})/C_{44} . \quad (4.12)$$

By a lengthy algebra, we have the elastic free energy including contributions from the electrostrictive effect in the Fourier representation:

$$\begin{aligned} F_{\mathrm{el}}+F_c&=\int d\mathbf{r}\{f_{\mathrm{el}}+f_c\}\\ &=-(1/2)\int d\mathbf{k}\Big[\sum_j G_j(\mathbf{k})G_j(-\mathbf{k})/d_j-D(\hat{\mathbf{k}})H(\mathbf{k})H(-\mathbf{k})\Big]\\ &=-(1/2)\sum_\rho\sum_\sigma\int d\mathbf{k}B_{\rho\sigma}(\hat{\mathbf{k}})g_\rho(\mathbf{k})g_\sigma(-\mathbf{k}) . \end{aligned} \quad (4.13)$$

The interaction matrix element $B_{\rho\sigma}(\hat{\mathbf{k}})$ is given by

$$B_{\rho\sigma}(\hat{\mathbf{k}})=\beta_{\rho\sigma}-D(\hat{\mathbf{k}})\theta_\rho\theta_\sigma , \quad (4.14)$$

where the matrix $\boldsymbol{\beta}$ is written as

$$\boldsymbol{\beta}=\begin{bmatrix} \hat{k}_x^2/d_x & 0 & 0 & 0 & \hat{k}_z\hat{k}_x/d_x & \hat{k}_x\hat{k}_y/d_x \\ 0 & \hat{k}_y^2/d_y & 0 & \hat{k}_y\hat{k}_z/d_y & 0 & \hat{k}_x\hat{k}_y/d_y \\ 0 & 0 & \hat{k}_z^2/d_z & \hat{k}_y\hat{k}_z/d_z & \hat{k}_x\hat{k}_z/d_z & 0 \\ 0 & 0 & \hat{k}_y\hat{k}_z/d_z & \hat{k}_y^2/d_z+\hat{k}_z^2/d_y & \hat{k}_x\hat{k}_y/d_z & \hat{k}_x\hat{k}_z/d_y \\ \hat{k}_z\hat{k}_x/d_x & 0 & \hat{k}_z\hat{k}_x/d_z & \hat{k}_x\hat{k}_y/d_z & \hat{k}_x^2/d_z+\hat{k}_z^2/d_x & \hat{k}_y\hat{k}_z/d_x \\ \hat{k}_x\hat{k}_y/d_x & \hat{k}_x\hat{k}_y/d_y & 0 & \hat{k}_x\hat{k}_z/d_y & \hat{k}_y\hat{k}_z/d_x & \hat{k}_x^2/d_y+\hat{k}_y^2/d_x \end{bmatrix} \quad (4.15)$$

and

$$\theta_1=\hat{k}_x^2/d_x , \quad (4.16a)$$

$$\theta_2=\hat{k}_y^2/d_y , \quad (4.16b)$$

$$\theta_3=\hat{k}_z^2/d_z , \quad (4.16c)$$

$$\theta_4=\hat{k}_y\hat{k}_z(1/d_y+1/d_z) , \quad (4.16d)$$

$$\theta_5=\hat{k}_x\hat{k}_z(1/d_x+1/d_z) , \quad (4.16e)$$

$$\theta_6=\hat{k}_x\hat{k}_y(1/d_x+1/d_y) . \quad (4.16f)$$

Using the inverse Fourier transformation, we have the long-range interaction between polarization fields eliminating the elastic field:

$$\begin{aligned} F_{\mathrm{lr}}&=F_{\mathrm{el}}+F_c\\ &=-2^{-1}\int\int d\mathbf{r}_1 d\mathbf{r}_2\sum_{\rho,\sigma=1}^{6}\Psi_{\rho\sigma}(\mathbf{r}_2-\mathbf{r}_1)Y_\rho(\mathbf{r}_1)Y_\sigma(\mathbf{r}_2) , \end{aligned} \quad (4.17)$$

where

$$\Psi_{\rho\sigma}(\mathbf{R})=(2\pi)^{-d}\int d\mathbf{k}\, A_{\rho\sigma}(\hat{\mathbf{k}})\exp[-i\mathbf{k}\cdot\mathbf{R}] \quad (4.18)$$

with

$$\begin{aligned} A_{\rho\rho}(\hat{\mathbf{k}})&=\hat{q}_{22}^2B_{\rho\rho}(\hat{\mathbf{k}})+2q_{12}\hat{q}_{22}\sum_{\sigma=1}^{3}B_{\rho\sigma}(\hat{\mathbf{k}})\\ &\quad+q_{12}^2\sum_{\rho,\sigma=1}^{3}\sum B_{\rho\sigma}(\hat{\mathbf{k}}) \quad (\rho=1,2,3) , \end{aligned} \quad (4.19)$$

$$\begin{aligned} A_{12}(\hat{\mathbf{k}})&=A_{21}(\hat{\mathbf{k}})\\ &=\hat{q}_{22}^2B_{12}(\hat{\mathbf{k}})-q_{12}\hat{q}_{22}\sum_{\rho=1}^{3}B_{\rho3}(\hat{\mathbf{k}})\\ &\quad+q_{11}q_{12}\sum_{\rho,\sigma=1}^{3}\sum B_{\rho\sigma}(\hat{\mathbf{k}}) , \end{aligned} \quad (4.20)$$

$$\begin{aligned} A_{13}(\hat{\mathbf{k}})&=A_{31}(\hat{\mathbf{k}})\\ &=\hat{q}_{22}^2B_{13}(\hat{\mathbf{k}})-q_{12}\hat{q}_{22}\sum_{\rho=1}^{3}B_{\rho2}(\hat{\mathbf{k}})\\ &\quad+q_{11}q_{12}\sum_{\rho,\sigma=1}^{3}\sum B_{\rho\sigma}(\hat{\mathbf{k}}) , \end{aligned} \quad (4.21)$$

$$\begin{aligned} A_{23}(\hat{\mathbf{k}})&=A_{32}(\hat{\mathbf{k}})\\ &=\hat{q}_{22}^2B_{23}(\hat{\mathbf{k}})-q_{12}\hat{q}_{22}\sum_{\rho=1}^{3}B_{\rho1}(\hat{\mathbf{k}})\\ &\quad+q_{11}q_{12}\sum_{\rho,\sigma=1}^{3}\sum B_{\rho\sigma}(\hat{\mathbf{k}}) , \end{aligned} \quad (4.22)$$

$$A_{1\sigma}(\hat{\mathbf{k}})=\hat{q}_{22}q_{44}B_{1\sigma}(\hat{\mathbf{k}})+q_{12}q_{44}\sum_{\rho=1}^{3}B_{\rho\sigma}(\hat{\mathbf{k}})\quad(\sigma=4,5,6)\ , \tag{4.23}$$

$$A_{2\sigma}(\hat{\mathbf{k}})=\hat{q}_{22}q_{44}B_{2\sigma}(\hat{\mathbf{k}})+q_{12}q_{44}\sum_{\rho=1}^{3}B_{\rho\sigma}(\hat{\mathbf{k}})\quad(\sigma=4,5,6)\ , \tag{4.24}$$

$$A_{3\sigma}(\hat{\mathbf{k}})=\hat{q}_{22}q_{44}B_{3\sigma}(\hat{\mathbf{k}})+q_{12}q_{44}\sum_{\rho=1}^{3}B_{\rho\sigma}(\hat{\mathbf{k}})\quad(\sigma=4,5,6)\ , \tag{4.25}$$

$$A_{\rho\sigma}(\hat{\mathbf{k}})=q_{44}^2B_{\rho\sigma}(\hat{\mathbf{k}})\quad(\rho,\sigma=4,5,6)\ , \tag{4.26}$$

and $Y_\rho(\mathbf{r})$ is the component of the vector $\mathbf{Y}$.

$$\mathbf{Y}(\mathbf{r})^t=[P_x(\mathbf{r})^2,P_y(\mathbf{r})^2,P_z(\mathbf{r})^2,P_y(\mathbf{r})\times P_z(\mathbf{r}),P_x(\mathbf{r})P_z(\mathbf{r}),P_x(\mathbf{r})P_y(\mathbf{r})]\ . \tag{4.27}$$

The function $A_{\rho\sigma}(\hat{\mathbf{k}})$ in the Fourier space depends on only the direction $\hat{\mathbf{k}}=\mathbf{k}/|\mathbf{k}|$. Finally, we obtain the real-space representation of the total free energy in a compact form as

$$F=\int d\mathbf{r}[f_{\text{eff}}+f_g]-2^{-1}\int\int d\mathbf{r}_1 d\mathbf{r}_2\sum_\rho\sum_\sigma\tilde{\Psi}_{\rho\sigma}(\mathbf{r}_2-\mathbf{r}_1)\times Y_\rho(\mathbf{r}_1)Y_\sigma(\mathbf{r}_2)\ , \tag{4.28}$$

where

$$f_{\text{eff}}(\{P\})=\alpha_1(P_x^2+P_y^2+P_z^2)+\alpha_{11}''(P_x^2+P_y^2+P_z^2)^2+\alpha_{12}''(P_x^2P_y^2+P_y^2P_z^2+P_z^2P_x^2)+\alpha_{111}(P_x^6+P_y^6+P_z^6)+\alpha_{112}[P_x^4(P_y^2+P_z^2)+P_y^4(P_z^2+P_x^2)+P_z^4(P_x^2+P_y^2)]+\alpha_{123}P_x^2P_y^2P_z^2 \tag{4.29}$$

with

$$\alpha_{11}''=\alpha_{11}-6^{-1}(\hat{v}_{11}\hat{q}_{11}^{\,2}+2\hat{v}_{22}\hat{q}_{22}^{\,2})\ , \tag{4.30a}$$

$$\alpha_{12}''=\alpha_{12}-2^{-1}(v_{44}q_{44}^2-2\hat{v}_{22}\hat{q}_{22}^{\,2})\ , \tag{4.30b}$$

and

$$\tilde{\Psi}_{\rho\sigma}(\mathbf{R})=(2\pi)^{-d}\int d\mathbf{k}[A_{\rho\sigma}(\hat{\mathbf{k}})-\langle A_{\rho\sigma}(\hat{\mathbf{k}})\rangle_{\text{an}}]\times\exp[-i\mathbf{k}\cdot\mathbf{R}]\ . \tag{4.31}$$

The angle average $\langle\cdots\rangle_{\text{an}}$ is used to avoid the divergence at $\mathbf{R}=0$. New parameters are given by

$$\hat{v}_{11}=v_{11}+2v_{12}\ , \tag{4.32a}$$

$$\hat{v}_{22}=v_{11}-v_{12}\ , \tag{4.32b}$$

and

$$v_{11}=\langle B_{11}(\hat{\mathbf{k}})\rangle_{\text{an}}\ , \tag{4.32c}$$

$$v_{12}=\langle B_{12}(\hat{\mathbf{k}})\rangle_{\text{an}}\ , \tag{4.32d}$$

$$v_{44}=\langle B_{44}(\hat{\mathbf{k}})\rangle_{\text{an}}\ . \tag{4.32e}$$

Since $A_{\rho\sigma}(\hat{\mathbf{k}})$ depends on only the direction $\hat{\mathbf{k}}$, the function $\tilde{\Psi}_{\rho\sigma}(\hat{\mathbf{R}})$ has the form

$$\tilde{\Psi}_{\rho\sigma}(\mathbf{R})=|\mathbf{R}|^{-d}\phi(\mathbf{R}/|\mathbf{R}|)\ , \tag{4.33}$$

where d is the dimensionality. The interaction term in the right-hand side of Eq. (4.28) is the anisotropic long-range interaction determined by the elastic and the electrostrictive property of the materials, that is, the phenomenological parameters included in $\tilde{\Psi}_{\rho\sigma}(\tilde{R})$ are C_{ij} and q_{ij}.

It should be noted that the effective free-energy density of Eq. (4.29) has the same form as Eq. (3.4) by replacing $\alpha_{11}'\rightarrow\alpha_{11}''$ and $\alpha_{12}'\rightarrow\alpha_{12}''$, namely $C_{ij}^{-1}\rightarrow v_{ij}$. The local strain field $u_\rho(\mathbf{r})$ ($\rho=1\sim6$) can be given by

$$u_\rho(\mathbf{r})=E_\rho(\mathbf{r})+\int d\mathbf{r}'\Big[\hat{q}_{22}\sum_{\sigma=1}^{3}\tilde{\psi}_{\rho\sigma}(\mathbf{r}'-\mathbf{r})Y_\sigma(\mathbf{r}')+q_{12}\sum_{\sigma=1}^{3}\tilde{\psi}_{\rho\sigma}(\mathbf{r}'-\mathbf{r})\sum_{\lambda=1}^{3}Y_\lambda(\mathbf{r}')+q_{44}\sum_{\sigma=4}^{6}\tilde{\psi}_{\rho\sigma}(\mathbf{r}'-\mathbf{r})Y_\sigma(\mathbf{r}')\Big]\ , \tag{4.34}$$

where

$$E_1(\mathbf{r})=Q_{11}'P_x(\mathbf{r})^2+Q_{12}'\{P_y(\mathbf{r})^2+P_z(\mathbf{r})^2\}\ , \tag{4.35a}$$

$$E_2(\mathbf{r})=Q_{11}'P_y(\mathbf{r})^2+Q_{12}'\{P_x(\mathbf{r})^2+P_z(\mathbf{r})^2\}\ , \tag{4.35b}$$

$$E_3(\mathbf{r})=Q_{11}'P_z(\mathbf{r})^2+Q_{12}'\{P_x(\mathbf{r})^2+P_y(\mathbf{r})^2\}\ , \tag{4.35c}$$

$$E_4(\mathbf{r})=Q_{44}'P_y(\mathbf{r})P_z(\mathbf{r})\ , \tag{4.35d}$$

$$E_5(\mathbf{r})=Q_{44}'P_x(\mathbf{r})P_z(\mathbf{r})\ , \tag{4.35e}$$

$$E_6(\mathbf{r})=Q_{44}'P_x(\mathbf{r})P_y(\mathbf{r})\ , \tag{4.35f}$$

and

$$\tilde{\psi}_{\rho\sigma}(\mathbf{R})=(2\pi)^{-d}\int d\mathbf{k}[B_{\rho\sigma}(\hat{\mathbf{k}})-\langle B_{\rho\sigma}(\hat{\mathbf{k}})\rangle_{\text{an}}]\times\exp[-i\mathbf{k}\cdot\mathbf{R}]\ , \tag{4.36}$$

$$Q_{11}'=3^{-1}(\hat{v}_{11}\hat{q}_{11}+2\hat{v}_{22}\hat{q}_{22})\ , \tag{4.37a}$$

$$Q_{12}'=3^{-1}(\hat{v}_{11}\hat{q}_{11}-\hat{v}_{22}\hat{q}_{22})\ , \tag{4.37b}$$

$$Q_{44}'=v_{44}q_{44}\ . \tag{4.37c}$$

Concerning the local strain field, the compatibility relations always hold since we obtained the local displacement field and then calculated the strain field and the stress field.

V. TIME-DEPENDENT GINZBURG-LANDAU EQUATION

The time evolution of the nonconserved order parameter $P(\mathbf{r},t)$ is determined by the time-dependent Ginzburg-Landau equation. Derivation of the dynamic equation which describes pattern formation of the ferroelectric domain structure, is based on the assumption that the relaxation of the polarization field $\mathbf{P}(\mathbf{r},t)$ is much "slower" compared to the elastic field at long wavelengths and the elastic field instantaneously relaxes to adjust to a given polarization configuration. The free-energy functional of Eq. (4.28) derived by eliminating elastic fields is used to obtain the dynamic equation. This is the adiabatic approximation. As was noted by Gunton, San Miguel, and Sahni,[24] the free-energy functional in the TDGL models is the coarse-grained free-energy functional, and the field variable is semimacroscopic variable. In this sense, the polarization field $P(\mathbf{r},t)$ in this paper should be regarded as semimacroscopic variable. In fact, the time scale of domain formation in $BaTiO_3$ is much slower (order of a minute or hour) compared to the microscopic relaxation process.[2,3]

The dynamic equation of polarization field is given by the following TDGL equation:

$$\frac{\partial}{\partial t}P_i(\mathbf{r},t)=-\Gamma\frac{\delta F}{\delta P_i(\mathbf{r})}+\xi_i(\mathbf{r},t)\ , \tag{5.1}$$

where F is the total free-energy functional given by Eq. (4.28) and Γ is a kinetic coefficient, and $\xi_i(\mathbf{r},t)$ is the Gaussian random force.

$$\langle \xi_i(\mathbf{r},t)\rangle=0\ , \tag{5.2a}$$

$$\langle \xi_i(\mathbf{r},t)\xi_j(\mathbf{r}',t')\rangle=2k_BT\Gamma\delta_{ij}\delta(\mathbf{r}-\mathbf{r}')\delta(t-t')\ . \tag{5.2b}$$

The functional derivative leads to the following equation:

$$-\frac{\partial}{\partial t}\mathbf{P}(\mathbf{r},t)=\Gamma\Lambda\mathbf{P}(\mathbf{r},t)-\xi(\mathbf{r},t)\ , \tag{5.3}$$

where the matrix Λ is given by

$$\Lambda=\begin{bmatrix}\Lambda_{xx} & \Lambda_{xy} & \Lambda_{xz}\\ \Lambda_{yx} & \Lambda_{yy} & \Lambda_{yz}\\ \Lambda_{zx} & \Lambda_{zy} & \Lambda_{zz}\end{bmatrix}\ , \tag{5.4}$$

with

$$\Lambda_{xx}=2\alpha_1+4\alpha_{11}''\mathbf{P}(\mathbf{r})^2+2\alpha_{12}''\{P_y(\mathbf{r})^2+P_z(\mathbf{r})^2\}+6\alpha_{111}P_x(\mathbf{r})^4+4\alpha_{112}P_x(\mathbf{r})^2\{P_y(\mathbf{r})^2+P_z(\mathbf{r})^2\}+2\alpha_{112}\{P_y(\mathbf{r})^4+P_z(\mathbf{r})^4\}$$
$$+2\alpha_{123}P_y(\mathbf{r})^2P_z(\mathbf{r})^2-G_{11}\frac{\partial^2}{\partial x^2}-(G_{44}+G_{44}')\left\{\frac{\partial^2}{\partial y^2}+\frac{\partial^2}{\partial z^2}\right\}-\int d\mathbf{r}'\left[2\sum_{\sigma=1}^{6}\tilde{\Psi}_{1\sigma}(\mathbf{r}'-\mathbf{r})Y_\sigma(\mathbf{r}')\right]\ , \tag{5.5}$$

$$\Lambda_{yy}=2\alpha_1+4\alpha_{11}''\mathbf{P}(\mathbf{r})^2+2\alpha_{12}''\{P_x(\mathbf{r})^2+P_z(\mathbf{r})^2\}+6\alpha_{111}P_y(\mathbf{r})^4+4\alpha_{112}P_y(\mathbf{r})^2\{P_x(\mathbf{r})^2+P_z(\mathbf{r})^2\}+2\alpha_{112}\{P_x(\mathbf{r})^4+P_z(\mathbf{r})^4\}$$
$$+2\alpha_{123}P_x(\mathbf{r})^2P_z(\mathbf{r})^2-G_{11}\frac{\partial^2}{\partial y^2}-(G_{44}+G_{44}')\left\{\frac{\partial^2}{\partial x^2}+\frac{\partial^2}{\partial z^2}\right\}-\int d\mathbf{r}'\left[2\sum_{\sigma=1}^{6}\tilde{\Psi}_{2\sigma}(\mathbf{r}'-\mathbf{r})Y_\sigma(\mathbf{r}')\right]\ , \tag{5.6}$$

$$\Lambda_{zz}=2\alpha_1+4\alpha_{11}''\mathbf{P}(\mathbf{r})^2+2\alpha_{12}''\{P_x(\mathbf{r})^2+P_y(\mathbf{r})^2\}+6\alpha_{111}P_z(\mathbf{r})^4+4\alpha_{112}P_z(\mathbf{r})^2\{P_x(\mathbf{r})^2+P_y(\mathbf{r})^2\}+2\alpha_{112}\{P_x(\mathbf{r})^4+P_y(\mathbf{r})^4\}$$
$$+2\alpha_{123}P_x(\mathbf{r})^2P_y(\mathbf{r})^2-G_{11}\frac{\partial^2}{\partial z^2}-(G_{44}+G_{44}')\left\{\frac{\partial^2}{\partial x^2}+\frac{\partial^2}{\partial y^2}\right\}-\int d\mathbf{r}'\left[2\sum_{\sigma=1}^{6}\tilde{\Psi}_{3\sigma}(\mathbf{r}'-\mathbf{r})Y_\sigma(\mathbf{r}')\right]\ , \tag{5.7}$$

$$\Lambda_{yz}=-(G_{12}+G_{44}-G_{44}')\frac{\partial^2}{\partial y\,\partial z}-\int d\mathbf{r}'\left[\sum_{\sigma=1}^{6}\tilde{\Psi}_{4\sigma}(\mathbf{r}'-\mathbf{r})Y_\sigma(\mathbf{r}')\right]\ , \tag{5.8}$$

$$\Lambda_{xz}=-(G_{12}+G_{44}-G_{44}')\frac{\partial^2}{\partial x\,\partial z}-\int d\mathbf{r}'\left[\sum_{\sigma=1}^{6}\tilde{\Psi}_{5\sigma}(\mathbf{r}'-\mathbf{r})Y_\sigma(\mathbf{r}')\right]\ , \tag{5.9}$$

$$\Lambda_{xy}=-(G_{12}+G_{44}-G_{44}')\frac{\partial^2}{\partial x\,\partial y}-\int d\mathbf{r}'\left[\sum_{\sigma=1}^{6}\tilde{\Psi}_{6\sigma}(\mathbf{r}'-\mathbf{r})Y_\sigma(\mathbf{r}')\right]\ . \tag{5.10}$$

The effect of the elastic strain on the formation of the ferroelectric domain structure is so complex that computer simulation plays a major role, although the three-dimensional simulation including the long-range interactions is difficult for CPU time at the present stage. We restrict ourselves to the use of a two-dimensional model, which may not always describe the real three-dimensional domain patterns, in particular, the structure of domains observed in the rhombohedral phase of the $Pb(Zr,Ti)O_3$ system,[25,26] which is essentially a three dimensional case.

VI. TWO-DIMENSIONAL TDGL MODEL

The two-dimensional version of Eq. (5.3) with the polarization $\mathbf{P}=(P_x,P_y)$ in (x,y) space can be written in a simpler fashion by suitable rescaling of the fields.

$$\tilde{\mathbf{r}}=\{|2\alpha_1|/G_{11}\}^{1/2}\mathbf{r}\ , \tag{6.1}$$

$$\tau=|2\alpha_1|\Gamma t\ , \tag{6.2}$$

$$\hat{\mathbf{P}}=\mathbf{P}/P_s\ , \tag{6.3}$$

$$\gamma_1 = 2\alpha''_{11} P_s^2 / |\alpha_1| \ , \tag{6.4}$$

$$\gamma_2 = 3\alpha_{111} P_s^4 / |\alpha_1| \ , \tag{6.5}$$

$$w_{\rho\sigma} = \tilde{\Psi}_{\rho\sigma} P_s^2 / |2\alpha_1| \ , \tag{6.6}$$

$$g_{44} = (G_{44} + G'_{44}) / G_{11} \ , \tag{6.7}$$

$$g_{14} = (G_{12} + G_{44} - G'_{44}) / G_{11} \ , \tag{6.8}$$

where P_s is the magnitude of the spontaneous polarization at a given temperature. We neglect the noise term, since, at low temperatures, the role of the noise term is thought to be very small and does not affect the late stages of the time evolution.[27] The resulting dimensionless equation is

$$-\frac{\partial}{\partial \tau} \hat{\mathbf{P}}(\tilde{\mathbf{r}}, \tau) = \Lambda \hat{\mathbf{P}}(\tilde{\mathbf{r}}, \tau) \ , \tag{6.9}$$

$$\Lambda = \begin{bmatrix} \Lambda_{xx} & \Lambda_{xy} \\ \Lambda_{xy} & \Lambda_{yy} \end{bmatrix} , \tag{6.10}$$

where

$$\begin{aligned} \Lambda_{xx} = & -1 + \gamma_1 \hat{\mathbf{P}}(\tilde{\mathbf{r}})^2 + 2^{-1}\gamma_1(\alpha''_{12}/\alpha''_{11})\hat{P}_y(\tilde{\mathbf{r}})^2 + \gamma_2 \hat{P}_x(\tilde{\mathbf{r}})^4 + 3^{-1}\gamma_2(\alpha_{112}/\alpha_{111})[2\hat{P}_x(\tilde{\mathbf{r}})^2\hat{P}_y(\tilde{\mathbf{r}})^2 + \hat{P}_y(\tilde{\mathbf{r}})^4] \\ & -(\partial^2/\partial \tilde{x}^2) - g_{44}(\partial^2/\partial \tilde{y}^2) - 2\int d\tilde{\mathbf{r}}'[w_{11}(\tilde{\mathbf{R}})\hat{P}_x(\tilde{\mathbf{r}}')^2 + w_{12}(\tilde{\mathbf{R}})\hat{P}_y(\tilde{\mathbf{r}}')^2 + w_{16}(\tilde{\mathbf{R}})\hat{P}_x(\tilde{\mathbf{r}}')\hat{P}_y(\tilde{\mathbf{r}}')] \ , \end{aligned} \tag{6.11}$$

$$\begin{aligned} \Lambda_{yy} = & -1 + \gamma_1 \hat{\mathbf{P}}(\tilde{\mathbf{r}})^2 + 2^{-1}\gamma_1(\alpha''_{12}/\alpha''_{11})\hat{P}_x(\tilde{\mathbf{r}})^2 + \gamma_2 \hat{P}_y(\tilde{\mathbf{r}})^4 + 3^{-1}\gamma_2(\alpha_{112}/\alpha_{111})[2\hat{P}_x(\tilde{\mathbf{r}})^2\hat{P}_y(\tilde{\mathbf{r}})^2 + \hat{P}_x(\tilde{\mathbf{r}})^4] \\ & -(\partial^2/\partial \tilde{y}^2) - g_{44}(\partial^2/\partial \tilde{x}^2) - 2\int d\tilde{\mathbf{r}}'[w_{12}(\tilde{\mathbf{R}})\hat{P}_x(\tilde{\mathbf{r}}')^2 + w_{22}(\tilde{\mathbf{R}})\hat{P}_y(\tilde{\mathbf{r}}')^2 + w_{26}(\tilde{\mathbf{R}})\hat{P}_x(\tilde{\mathbf{r}}')\hat{P}_y(\tilde{\mathbf{r}}')] \ , \end{aligned} \tag{6.12}$$

$$\Lambda_{xy} = -g_{14}(\partial^2/\partial \tilde{x}\partial \tilde{y}) - \int d\tilde{\mathbf{r}}'[w_{66}(\tilde{\mathbf{R}})P_x(\tilde{\mathbf{r}}')\hat{P}_y(\tilde{\mathbf{r}}') + w_{16}(\tilde{\mathbf{R}})\hat{P}_x(\tilde{\mathbf{r}}')^2 + w_{26}(\tilde{\mathbf{R}})\hat{P}_y(\tilde{\mathbf{r}}')^2] \tag{6.13}$$

with $\tilde{\mathbf{R}} = \tilde{\mathbf{r}}' - \tilde{\mathbf{r}}$. Simulations will be done at low temperatures sufficiently below the transition temperature, we assumed $\alpha_1 = -|\alpha_1|$.

In order to clarify the elastic long-range interaction in real space and to carry out the numerical simulation for a two-dimensional space, the anisotropic long-range interaction $w_{\rho\sigma}(\tilde{\mathbf{R}})$ should be obtained as a function of $|\tilde{\mathbf{R}}|^{-2}$ and directional cosines $\hat{x} = \tilde{R}_x / |\tilde{\mathbf{R}}|$ and $\hat{y} = \tilde{R}_y / |\tilde{\mathbf{R}}|$ ($\hat{x}^2 + \hat{y}^2 = 1$) explicitly. In general, we should determine the habit plane in $\mathbf{k}$ space by the diagonalization of interaction matrix $A_{\rho\sigma}(\hat{\mathbf{k}})$ in Eq. (4.18), that is, the direction of the energy minimum with respect to the elastic free energy including the electrostrictive term. As was noted in the introduction, the twin plates are $\{110\}$ in the tetragonal $BaTiO_3$ and $Pb(Zr,Ti)O_3$. In the case of the present two-dimensional model, for simplicity, we use Taylor's expansion of $A_{\rho\sigma}$ with respect to the [11] direction in $\mathbf{k}$ space up to fourth order of directional cosines. The inverse Fourier transformation[23,28,29] and lengthy algebra yields the elastic long-range interactions $w_{\rho\sigma}(R)$ in the form:

$$w_{11}(\tilde{\mathbf{R}}) = w_0(1-2\hat{x}^2)/\tilde{R}^2 + w_1(1/8 - \hat{x}^2\hat{y}^2)/\tilde{R}^2 \ , \tag{6.14}$$

$$w_{22}(\tilde{\mathbf{R}}) = w_0(1-2\hat{y}^2)/\tilde{R}^2 + w_1(1/8 - \hat{x}^2\hat{y}^2)/\tilde{R}^2 \ , \tag{6.15}$$

$$w_{12}(\tilde{\mathbf{R}}) = w_2(1/8 - \hat{x}^2\hat{y}^2)/\tilde{R}^2 \ , \tag{6.16}$$

$$w_{16}(\tilde{\mathbf{R}}) = -w_3\hat{x}\hat{y}/\tilde{R}^2 - w_4\hat{x}\hat{y}(1-2\hat{x}^2)/\tilde{R}^2 \ , \tag{6.17}$$

$$w_{26}(\tilde{\mathbf{R}}) = -w_3\hat{x}\hat{y}/\tilde{R}^2 - w_4\hat{x}\hat{y}(1-2\hat{y}^2)/\tilde{R}^2 \ , \tag{6.18}$$

$$w_{66}(\tilde{\mathbf{R}}) = w_5(1/8 - \hat{x}^2\hat{y}^2)/\tilde{R}^2 \ , \tag{6.19}$$

where constant parameters w_j ($j = 0, 1, \ldots, 5$) are given by

$$w_0 = J(2-\eta)(q_{11}^2 - q_{12}^2)/2\pi\hat{C}_0 \ , \tag{6.20a}$$

$$\begin{aligned} w_1 = J(2/\pi)[& -(\hat{q}_{22}^2/\hat{C}_0)\{2\eta(1+2\hat{C}_1^2/\hat{C}_0\hat{C}_{22}) \\ & +(2-\eta)^2\hat{C}_1/\hat{C}_{22}\} \\ & -4\eta q_{11}q_{12}\hat{C}_{22}/\hat{C}_0^2] \ , \end{aligned} \tag{6.20b}$$

$$\begin{aligned} w_2 = J(2/\pi)[& \hat{q}_{22}^2(\hat{C}_1/\hat{C}_0\hat{C}_{22})\{4\eta(1-\hat{C}_1/\hat{C}_0)+(2-\eta)^2\} \\ & -4\eta q_{11}q_{12}\hat{C}_{22}/\hat{C}_0^2] \ , \end{aligned} \tag{6.20c}$$

$$w_3 = J(2/\pi)q_{44}(q_{11}+q_{12})/\hat{C}_0 \ , \tag{6.20d}$$

$$w_4 = J(2/\pi)[-q_{44}\hat{q}_{22}(\eta + 4\hat{C}_1/\hat{C}_{22})/\hat{C}_0] \ , \tag{6.20e}$$

$$\begin{aligned} w_5 = J(2/\pi)[& q_{44}^2\hat{C}_{22}^{-1}\{4\eta^2\hat{C}_{22}/\hat{C}_0 + 16\hat{C}_1/\hat{C}_0 \\ & +4\eta(1-4\hat{C}_1^2/\hat{C}_0^2)\}] \ , \end{aligned} \tag{6.20f}$$

with

$$J = P_s^2/|2\alpha_1| \ , \tag{6.21}$$

$$\eta = (C_{11} - C_{12} - 2C_{44})/(C_{11} - C_{12}) \ , \tag{6.22}$$

$$\hat{C}_0 = C_{11} + C_{12} + 2C_{44} \ , \tag{6.23}$$

$$\hat{C}_1 = C_{12} + C_{44} \ . \tag{6.24}$$

All parameters appearing in Eqs. (6.9)–(6.19) are dimensionless and order of unity. We chose the values of phenomenological parameters g_{14} and g_{44} so as to appear 90° domain, and others were roughly estimated from the ex-

TABLE I. Values of parameters used in the calculation.

g_{14}	g_{44}	γ_1	γ_2	$\alpha''_{12}/\alpha''_{11}$	$\alpha_{112}/\alpha_{111}$
1.90	1.00	−1.18	2.50	−20.0	5.10
w_0	w_1	w_2	w_3	w_4	w_5
0.14	−4.07	4.13	0.04	−0.25	0.38

perimental data of $BaTiO_3$ (Ref. 30) (Table I), but we didn't fit precisely these parameters to each physical quantities as has been done in the equilibrium theory.[31] We will give precise simulations for $BaTiO_3$ in a separate paper.

Numerically solving Eq. (6.9) is performed by a finite difference scheme for both the spatial and temporal derivatives. The spatial discretization is achieved by replacing the continuous space of position vector $\tilde{\mathbf{r}}=(\tilde{x},\tilde{y})$ by a square lattice with $N=L^2$ sites and lattice spacing Δx. It is necessary to choose the appropriate values of Δx and the time step $\Delta\tau$ for the stability of the numerical integration. We use in our simulation $L=128$, $\Delta x=0.3$, and $\Delta\tau=0.005$ with cyclic boundary condition. The initial configuration of the local polarization vector $\hat{\mathbf{P}}(\tilde{\mathbf{r}},0)$ is chosen to be uniformly distributed, where the mean

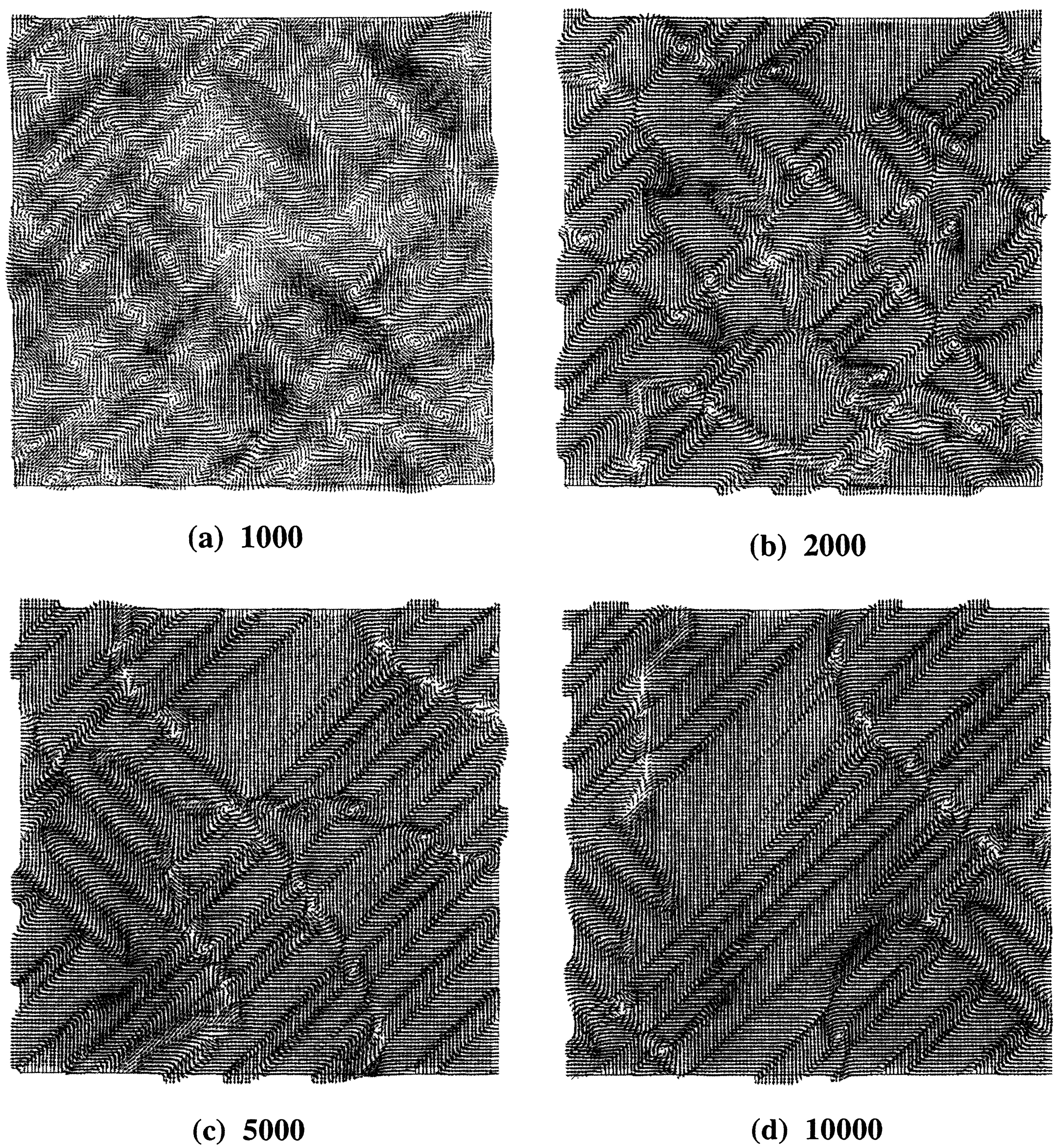

(a) 1000 (b) 2000 (c) 5000 (d) 10000

FIG. 1. Time evolution of 90° twin structure in a two-dimensional model including the elastic long-range interaction. The maximum value of normalized spontaneous polarization is 0.927. The numbers below the figures are the time steps after the quench.

value is zero vector and the standard deviation is 0.01 for $\hat{P}_x$ and $\hat{P}_y$. The square area of 30×30 lattice points around the position $\mathbf{\tilde{r}}$ is taken into account in the integral of the long-range interactions $w_{\rho\sigma}(\mathbf{\tilde{r}}'-\mathbf{\tilde{r}})$ with respect to $\mathbf{\tilde{r}}'$ in Eqs. (6.11)–(6.13).

Figure 1 shows the time evolution of 90° domain structure along the [11] direction calculated at various time steps. In order to clarify the effect of elastic long-range interactions, we show the results of the simulation using the same values of parameters only without the elastic long-range interactions ($w_0=w_1=w_2=w_3=w_4=w_5=0$) in Fig. 2, which corresponds to the stress-free state. In an early stage of domain formation (1000 and 2000 steps), the gradient energy terms is dominant to form 90° domain patterns. Similar patterns were obtained at 1000 and 2000 steps in Figs. 1 and 2.

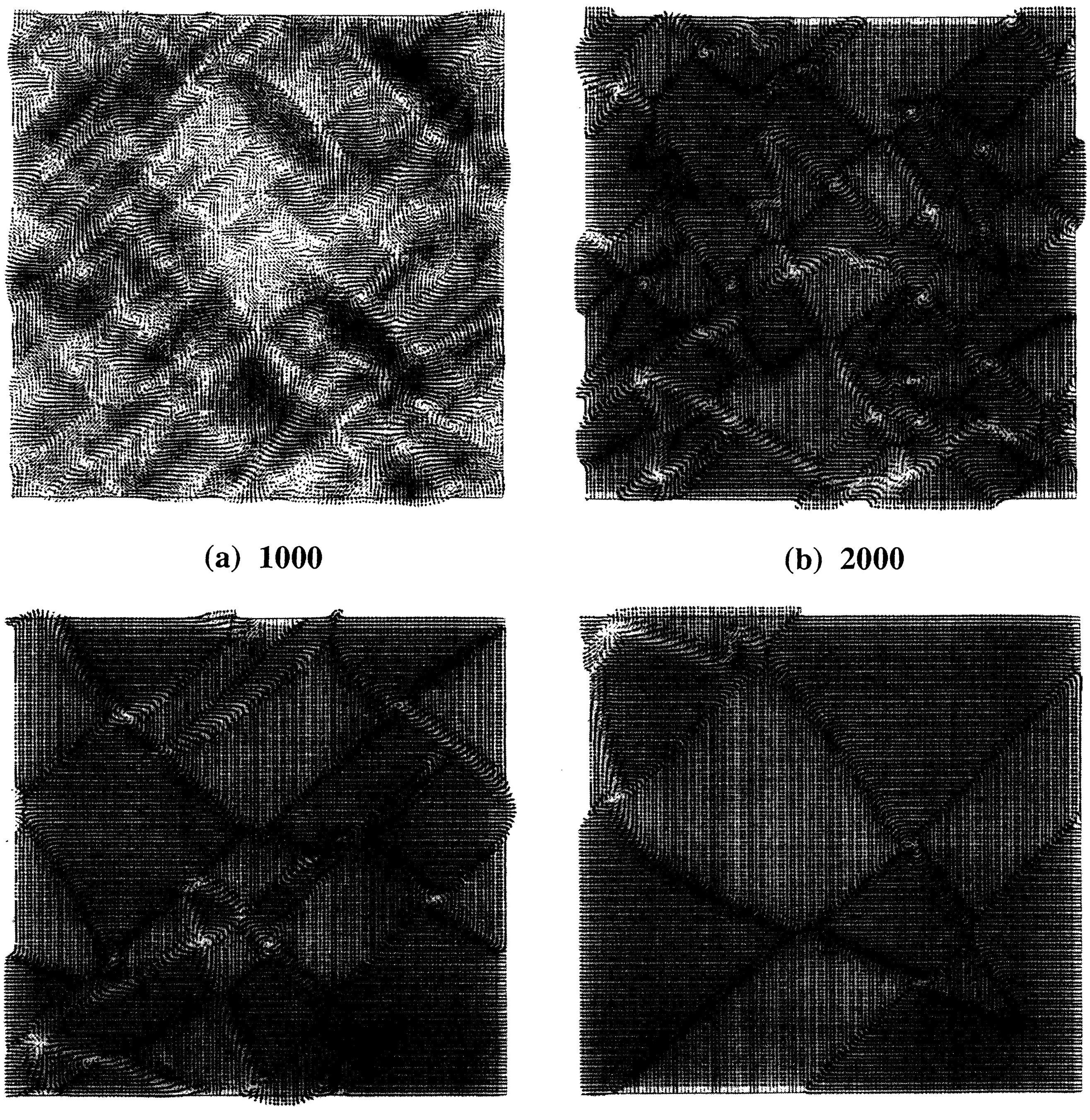

(a) 1000

(b) 2000

(c) 5000

(d) 10000

FIG. 2. Time evolution of 90° twin structure in a two-dimensional model without elastic long-range interaction, which corresponds to the case of stress free state. The maximum value of normalized spontaneous polarization is 1.00. The numbers below the figures are the time steps after the quench.

On the contrary, in the late stage, the effect of elastic long-range interactions appears as shown in Figs. 1(c) and 1(d). The growth of the width of domains is drastically slowed down due to the presence of the elastic constraint. Because the elastic long-range interaction in Eq. (4.28) is a fourth-order interaction with respect to the polarization vector, so that the effect of elastic constraint appears after that the magnitude of spontaneous polarization approaches its saturated value, this is apparently a nonlinear effect in the formation of twin structures. In fact, the case of the stress-free state (Fig. 2), the continuous growth of domain patterns with similar figures can be seen. The maximum values of the normalized spontaneous polarization at each lattice site in the late stage are 0.927 in the case including elastic long-range interaction and 1.00 in the case without it, where we chose the values of parameters so that the normalized polarization saturates to unity in the case without elastic long-range interaction.

The domain structure obtained in Fig. 1 is simple lamellar twinning. There are two typical patterns of 90° twins observed in a ceramic crystallite (single grain), herringbone and simple lamellar patterns. Arlt[5] showed that a crystallite (grain) clamped in two dimensions, such as the surface of polycrystal or thin layer, has a simple lamellar twinning in the tetragonal $BaTiO_3$. Our result, based on the two-dimensional model, quite reasonably explains, the appearance of lamellar twinning in a two-dimensional clamped surface, and the reason why the domain growth of 90° twins is frozen as observed in ceramics compared to single crystals.

VII. SUMMARY AND CONCLUSION

Theory and simulation were presented to describe the effect of elastic strain on the tetragonal twin structures of ferroelectric perovskites. The effective free energy including elastic long-range interactions was derived for polarization fields which is coherently induced by polarization inhomogeneities. Computer simulations for the two-dimensional space showed that the elastic long-range interactions between polarization fields give the lamellar twin structure of 90° domain and the frozen patterns experimentally observed in the tetragonal $BaTiO_3$ ceramics. It is interesting that numerical simulations based on the present method can be applicable to the study of the kinetics of domain-wall motion and ferroelectric characteristics, such as hysteresis loop, etc., which have long been unsolved problems in the microscopic level due to their complexity, although the technological importance is increasing more and more recently. Theory presented here and computer simulations by an extensive use of the resources of both memory and CPU of a powerful supercomputer will give a three-dimensional solution of the formation of ferroelectric domain structure and ferroelectric characteristics due to its domain motion.

ACKNOWLEDGMENT

We thank M. Yamaguchi for an assistance of numerical calculations.

[1] M. C. Mcquarrie, J. Appl. Phys. **24**, 1334 (1953).

[2] S. Ikegami and I. Ueda, J. Phys. Soc. Jpn. **22**, 725 (1967).

[3] R. C. Bradt and G. S. Ansell, J. Am. Ceram. Soc. **52**, 192 (1969).

[4] H. Dederichs and G. Arlt, Ferroelectrics **68**, 281 (1986).

[5] G. Arlt, J. Mater. Sci. **25**, 2655 (1990).

[6] R. C. De Vries and J. E. Burke, J. Am. Ceram. Soc. **40**, 200 (1957).

[7] G. Arlt and P. Sasko, J. Appl. Phys. **51**, 4956 (1980).

[8] Y. H. Hu, H. M. Chan, Z. X. Wen, and M. P. Harmer, J. Am. Ceram. Soc. **69**, 594 (1986).

[9] R. Gerson, J. Appl. Phys. **31**, 188 (1960).

[10] E. K. W. Goo, R. K. Mishra, and G. Thomas, J. Appl. Phys. **52**, 2940 (1981).

[11] C. A. Randall, D. J. Barber, and R. W. Whatmore, J. Mater. Sci. **22**, 925 (1987).

[12] P. G. Lucuta, J. Am. Ceram. Soc. **72**, 933 (1989).

[13] B. G. Demczyk, R. S. Rai, and G. Thomas, J. Am. Ceram. Soc. **73**, 615 (1990).

[14] E. I. Eknadiosiants *et al.*, Ferroelectrics **111**, 283 (1990).

[15] W. Cao and L. E. Cross, Phys. Rev. B **44**, 5 (1991).

[16] G. R. Barsch and J. K. Krumhansl, Phys. Rev. Lett. **53**, 1069 (1984).

[17] B. Horovitz, G. R. Barsch, and J. A. Krumhansl, Phys. Rev. B **43**, 1021 (1991).

[18] H. Nishimori and A. Onuki, Phys. Rev. B **42**, 980 (1990).

[19] H. Nishimori and A. Onuki, J. Phys. Soc. Jpn. **60**, 1209 (1991).

[20] A. Onuki and H. Nishimori, Phys. Rev. B **43**, 13 649 (1991).

[21] S. Nambu and M. Oiji, J. Am. Ceram. Soc. **74**, 1910 (1991).

[22] S. Nambu, A. Sato, and D. A. Sagala, J. Am. Ceram. Soc. **75**, 1906 (1992).

[23] S. Nambu and A. Sato, J. Am. Ceram. Soc. **76**, 1978 (1993).

[24] J. D. Gunton, M. San Miguel, and P. S. Sahni, in *Phase Transitions and Critical Phenomena,* edited by C. Domb and J. L. Lebowitz (Academic, New York, 1983), Vol. 8.

[25] C. A. Randall, D. J. Barber, and R. W. Whatmore, J. Mater. Sci. **22**, 925 (1987).

[26] E. I. Eknadiosiants, V. Z. Borodin, V. G. Smotrakov, V. V. Eremkin, and A. N. Pinskaya, Ferroelectrics **111**, 283 (1990).

[27] T. M. Rogers, K. R. Elder, and R. C. Desai, Phys. Rev. B **37**, 9638 (1988).

[28] A. G. Khachaturyan, *Theory of Structural Transformations in Solids* (Wiley, New York, 1983).

[29] H. Yamanouchi and D. de Fontaine, Acta Metall. **14**, 1295 (1979).

[30] *Elastic, Piezoelectric, Pyroelectric Piezooptic, Elektrooptic Constants, and Nonlinear Dielectric Susceptibilities of Crystals,* edited by K. H. Hellwege and A. M. Hellwege, Landolt-Bořnstein, New Series, Group 3, Vol. 11 (Springer-Verlag, Berlin, 1979); *Ferroelectrics and Related Substances,* edited by K. H. Hellwege and A. M. Hellwege, Landolt-Bořnstein, New Series, Group 3, Vol. 16, Pt. a (Springer-Verlag, Berlin, 1982).

[31] A. F. Devonshire, Philos. Mag. **40**, 1040 (1949).

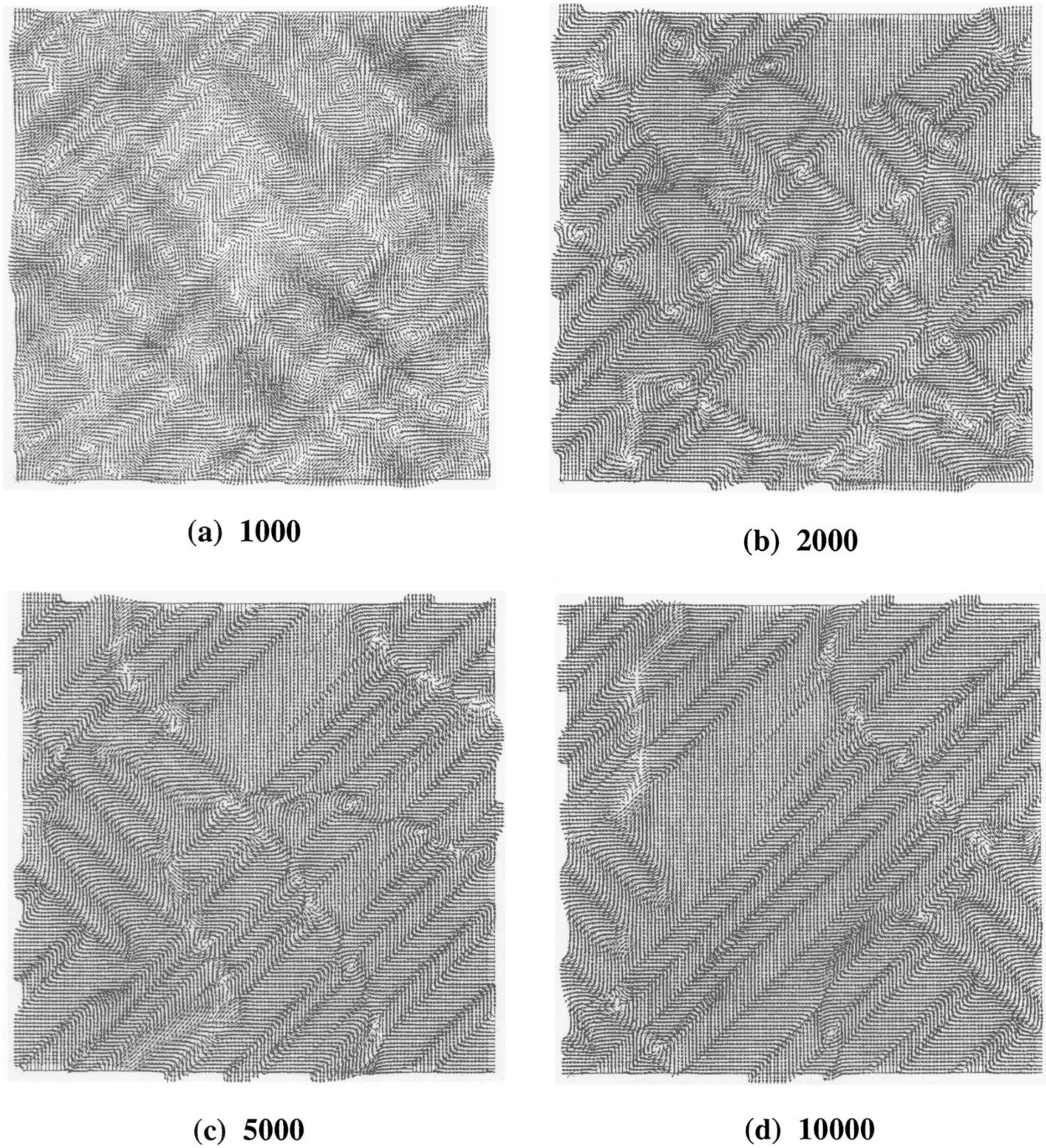

FIG. 1. Time evolution of 90° twin structure in a two-dimensional model including the elastic long-range interaction. The maximum value of normalized spontaneous polarization is 0.927. The numbers below the figures are the time steps after the quench.

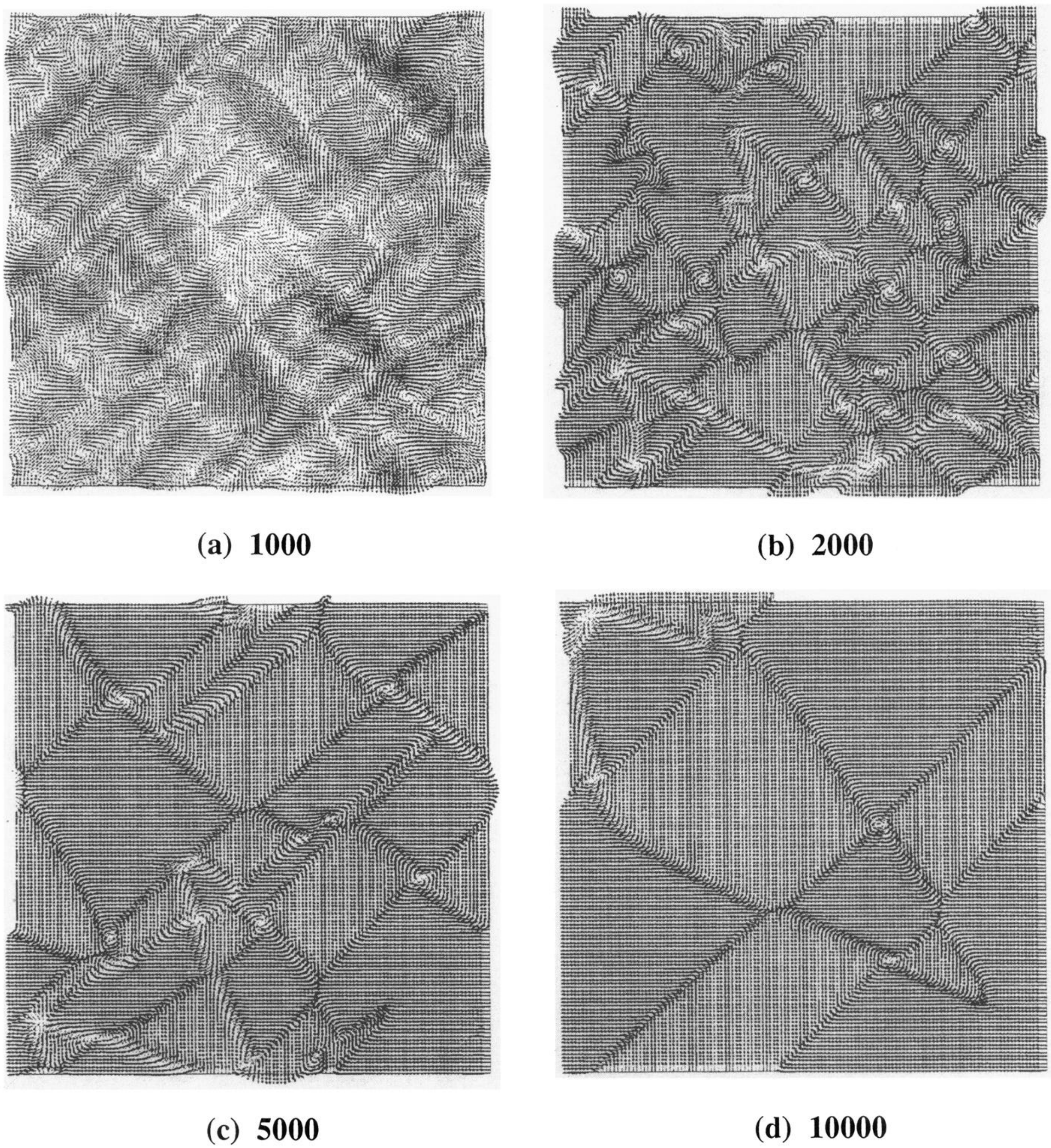

FIG. 2. Time evolution of 90° twin structure in a two-dimensional model without elastic long-range interaction, which corresponds to the case of stress free state. The maximum value of normalized spontaneous polarization is 1.00. The numbers below the figures are the time steps after the quench.